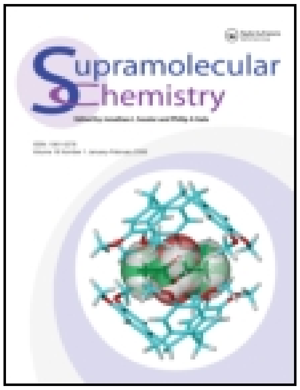

Supramolecular Chemistry
Publication details, including instructions for authors and subscription information:
http://www.tandfonline.com/loi/gsch20

Supramolecular assemblies of crown-substituted dinickel and dicobalt complexes with guest cation binding

Hisashi Shimakoshi [a], Daisuke Maeda [a] & Yoshio Hisaeda [a] [b]

[a] Department of Chemistry and Biochemistry, Graduate School of Engineering, Kyushu University, Fukuoka, 819-0395, Japan

[b] International Research Center for Molecular Systems (IRCMS), Kyushu University, Fukuoka, 819-0395, Japan

To cite this article: Hisashi Shimakoshi, Daisuke Maeda & Yoshio Hisaeda (2011): Supramolecular assemblies of crown-substituted dinickel and dicobalt complexes with guest cation binding, Supramolecular Chemistry, 23:01-02, 131-139

To link to this article: http://dx.doi.org/10.1080/10610278.2010.514910

Supramolecular Chemistry
Vol. 23, Nos. 1–2, January–February 2011, 131–139

Taylor & Francis
Taylor & Francis Group

Supramolecular assemblies of crown-substituted dinickel and dicobalt complexes with guest cation binding

Hisashi Shimakoshi[a], Daisuke Maeda[a] and Yoshio Hisaeda[ab]*

[a]*Department of Chemistry and Biochemistry, Graduate School of Engineering, Kyushu University, Fukuoka 819-0395, Japan;* [b]*International Research Center for Molecular Systems (IRCMS), Kyushu University, Fukuoka 819-0395, Japan*

(*Received 7 June 2010; final version received 5 August 2010*)

A new macrocyclic ligand (**L1**) having four crown ether moieties at the peripheral position was synthesised by a conventional Schiff-base condensation reaction. The corresponding dinickel (**1**) and dicobalt (**2**) complexes formed a unique face-to-face dimerised structure by complexation with a Cs^+ ion, which was characterised by ^1H NMR, UV–vis and electrospray ionisation (ESI)-MS. Multi-sandwich structures consist of a 2:1 interaction of the benzo-18-crown-6 ether with the Cs^+ ion affording a significantly high overall formation constant ($K_{all} = 25.9 \pm 0.9$ at 298 K). The redox behaviour of the assembled structure of the dicobalt complex was investigated by cyclic voltammetry. In the dimerised structure, two sequential reductions ascribed to the $Co^{II}Co^{II}/Co^{II}Co^{I}$ and $Co^{II}Co^{I}/Co^{I}Co^{I}$ couples were observed at -1.13 V (E_1) and -1.36 V (E_2) vs. Ag/AgCl, and both potentials were separated by $E = E_1 - E_2 = 0.23$ V. A mixed valence state ($Co^{II}Co^{I}$) was stabilised in the complex with the comproportionation constant $K_{com} = 7.7 \times 10^3$ at 298 K.

Keywords: crown ether; Schiff-base; dinuclear complex; face-to-face dimerised structure; mixed valence state

Introduction

The host–guest interaction is an important tool for the construction of a supramolecular assembly of various functional materials, such as a metal complex, dye and catalyst (*1–3*). A well-designed assembled structure provides a unique function in supramolecular chemistry. In this area, the properties of the crown ether for host–guest interactions are some of the most useful tools for molecular assembly (*4*, *5*). Therefore, many studies have emerged in the past two decades using the crown ether moiety for this purpose. To utilise the cation-binding property of the crown ether for construction of the assembled structure, crown ether moieties were introduced at the peripheral position of the desired molecule, such as a porphyrin, phthalocyanine or other compounds (*6–21*). In these studies, a unique face-to-face structure was constructed based on a sandwich-type interaction between two moles of the crown ether and cation as shown in Figure 1.

Recently, we reported the syntheses of a variety of dicobalt complexes with Schiff-base macrocyclic ligands (*22–28*). The Schiff-base macrocycle is a useful molecule for constructing various metal complexes with the desired structure (*29–34*). Especially, the multi-metallic complex of the Schiff-base macrocycle has been developed in the fields of catalytic chemistry, host–guest chemistry and bioinorganic chemistry (*35–38*). Furthermore, the supramolecular assembly of the Schiff-base macrocycle has been reported in recent years (*39–42*). This approach will open the door to extend the Schiff-base macrocycle into new molecular systems. To develop this approach, we introduced the crown ether moiety into a Schiff-base macrocycle. In the molecule, the formation of a unique sandwich-type structure in dimetallic complexes ($Ni^{II}Ni^{II}$, $Co^{II}Co^{II}$) will be expected. The syntheses and supramolecular assemblies of dimetallic complexes caused by the host–guest interaction of crown ether moieties and cations are reported in this paper.

Results and discussion

Synthesis of dicobalt and dinickel complexes

A dinucleating ligand (**L1**) having four crown ether moieties was synthesised by the conventional Schiff-base condensation reaction between the 1,2,4,5-tetraaminobenzene tetrahydrochloride and salicylaldehyde derivative (4′-hydroxy-5′-formylbenzo-18-crown-6 ether) having a benzo-18-crown-6 ether moiety as shown in Scheme 1. The compound was characterised by IR, UV–vis, NMR, electrospray ionisation (ESI)-MS and elemental analysis. The characteristic NMR signal ascribed to the phenolic protons with strong hydrogen bonding (—PhOH···N═C—) appeared at 13.3 ppm, and the IR analysis showed an intense ν(C═N) band at 1620 cm^{-1} (*27*). ESI-MS showed a strong peak at $m/z = 1514.2$ ascribed to $M + Na^+$. The synthesised Schiff-base ligand having two N_2O_2 cores was

---

*Corresponding author. Email: yhisatcm@mail.cstm.kyushu-u.ac.jp

ISSN 1061-0278 print/ISSN 1029-0478 online

DOI: 10.1080/10610278.2010.514910
http://www.informaworld.com

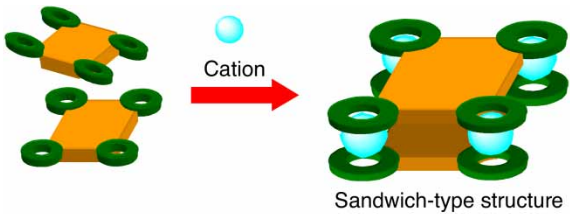

Figure 1. Schematic representation of the cation-induced supramolecular assembly of the crown ether-substituted molecule.

suitable for accommodating two metal ions. The corresponding dinickel and dicobalt complexes were synthesised by the reaction of **L1** with nickel(II) acetate and cobalt(II) acetate, respectively. The diamagnetic nickel (II) complex **1** showed a well-defined NMR spectrum at 3–8.5 ppm, and the phenolic protons of **L1** disappeared by complexation with the nickel ions. A band assignable to the C=N vibration of the coordinated azomethine group appeared at 1600 cm^{-1}, which is shifted to a lower energy by 20 cm^{-1} compared to that of **L1**, indicating that the ligand is coordinated to the nickel ion through the nitrogen atoms of the azomethine group (*27*). ESI-MS shows a strong peak at $m/z = 1628.1$ ascribed to $M + Na^+$. The dicobalt complex **2** was synthesised in an almost similar manner to that for **1** under anaerobic conditions and was characterised by elemental analysis, IR, UV–vis and ESI-MS (see Experimental section). According to these spectroscopic data, both dimetal complexes (**1**, $Ni^{II}Ni^{II}$ and **2**, $Co^{II}Co^{II}$) of **L1** having the benzo-18-crown-6 ether moiety were successfully synthesised. The supramolecular assemblies of **1** and **2** with guest cation binding were investigated in detail.

Supramolecular assemblies of 1 and 2

^{1}H NMR and ESI-MS studies

The complexation ability of **1** with alkali metal cations (K^+ and Cs^+) was analysed by ^{1}H NMR in dimethyl sulphoxide-d_6 (DMSO-d_6). Upon complexation, the peaks for the crown ether bridge protons shifted downfield upon

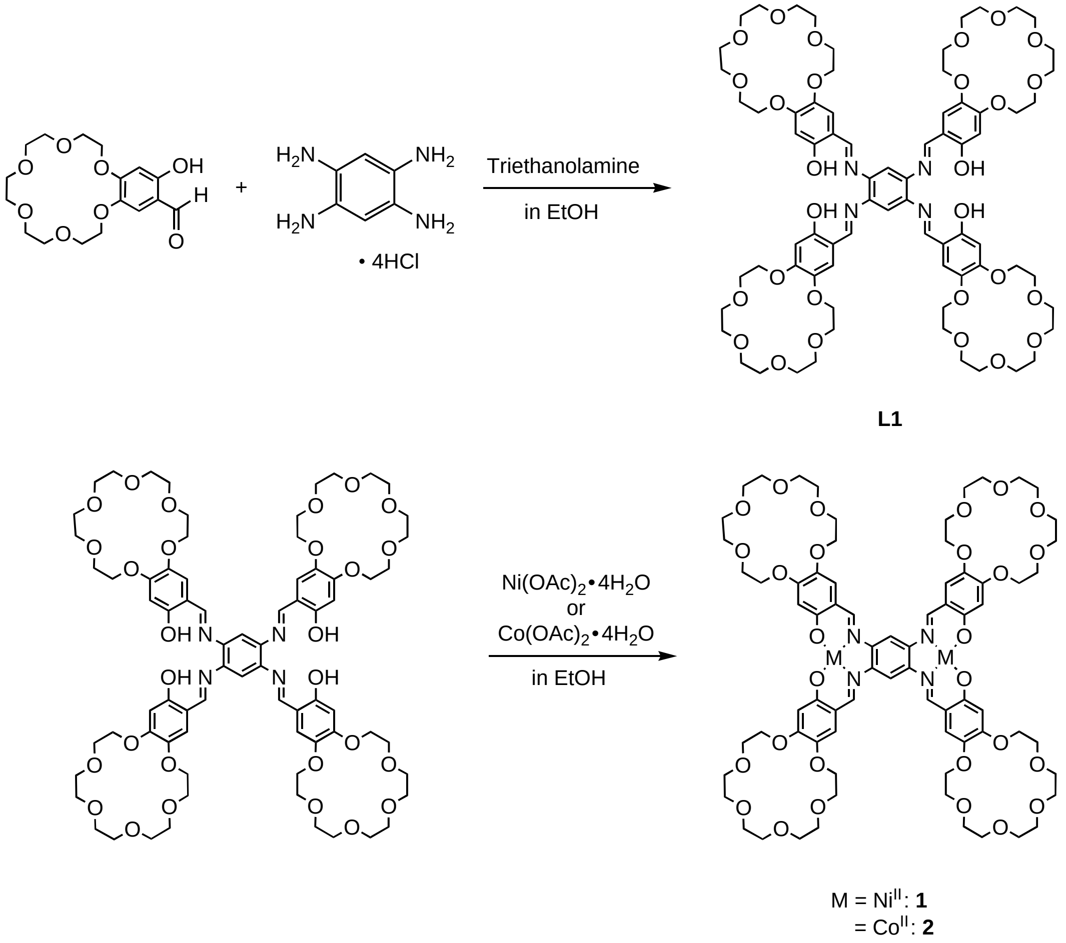

Scheme 1. Synthesis of dinickel and dicobalt complexes.

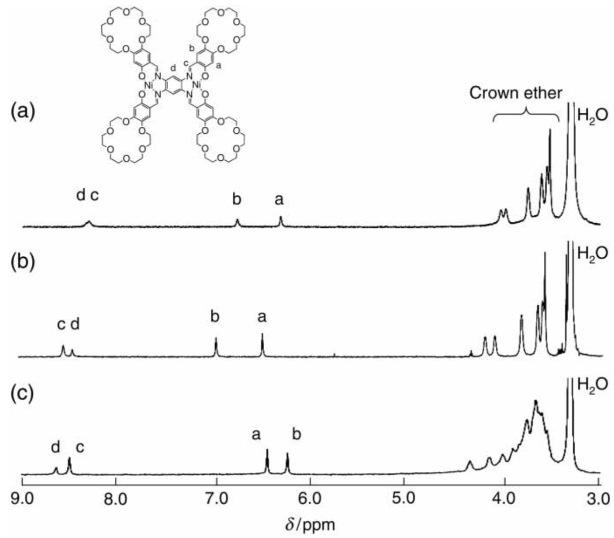

Figure 2. ^{1}H NMR spectra of **1** (1.0×10^{-3} M) in DMSO-d_6 at 298 K. (a) **1**, (b) **1** + 4 equiv. mol of $KClO_4$ and (c) **1** + 2 equiv. mol of $CsClO_4$.

addition of both the K^+ and Cs^+ ions. In contrast, the peak assignable to the *o*-position of the benzene ring (peak b in Figure 2) shifted in a different direction upon addition of the K^+ and Cs^+ ions; an unusual upfield shift was observed for the Cs^+ ion binding as shown in Figure 3. These spectral changes indicate that different supramolecular structures in **1** were formed that were dependent on the alkali cations. A possible explanation for this upfield shift of the b proton upon the Cs^+ ion addition is due to the face-to face assembled structure in **1**. The face-to-face structure positioned the b proton near an opposite benzene ring of **1** and disposed the b proton in the shielding area. As the four crown ether moieties are substituted on the same plane of **1**, the face-to-face dimerised complex should have high a symmetrical structure. Therefore, no ROESY peak other than those expected in the same basic macrocycle (the protons c and d, c and b) was observed in **1** with the assembled structure. ESI-MS provided direct evidence for the formation of the assembled structure for the Cs^+ ion binding. An intense peak at 935.44 ascribed to the sandwich structure of **1** with Cs^+ ions ($[\mathbf{1}_2Cs_4]^{4+}$, M-4ClO_4) was obtained in the presence of 2 equiv. mol of $CsClO_4$ with the satisfied isotope pattern as shown in Figure 4(a). As the benzo-18-crown-6 ether forms a sandwich structure with the Cs^+ ion (*1*, *2*), the complex **1** provided a stable 2:4 assembled structure due to the Cs^+ ion binding (Scheme 2). A similar 2:4 assembled structure of **2** by Cs^+ ion binding was also confirmed by the ESI-MS analysis, $m/z = 935.75$ ($[\mathbf{2}_2Cs_4]^{4+}$, M-4ClO_4) as shown in Figure 4(b). In contrast, peaks at 841.50 and 1643.98 ascribed to $[\mathbf{1} + 2K]^{2+}$ (M-2ClO_4) and $[\mathbf{1} + K]^+$ (M-ClO_4) were obtained in the presence of 4 equiv. mol of $KClO_4$ as shown in Figure 4(c). The peak which was

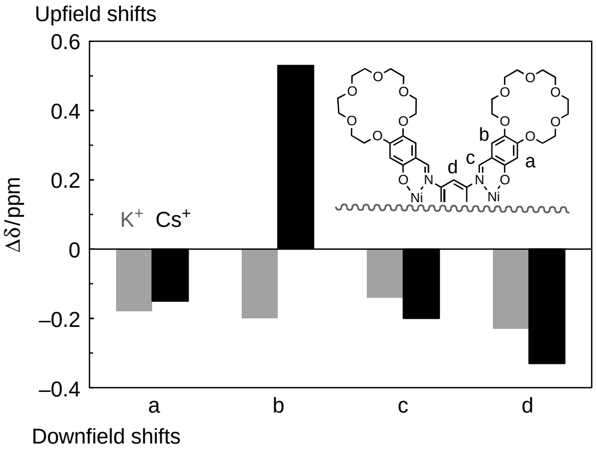

Figure 3. Complexation-induced shifts (Δ*δ*) of **1** complexed with $KClO_4$ (grey bar) and $CsClO_4$ (black bar). The positive and negative values represent upfield and downfield shifts, respectively.

ascribed to 1:4 structure of **1** with K^+ ion was not observed even in low temperature (~233 K) and/or in the presence of excess amount of $KClO_4$ (40 equiv. mol) since the host–

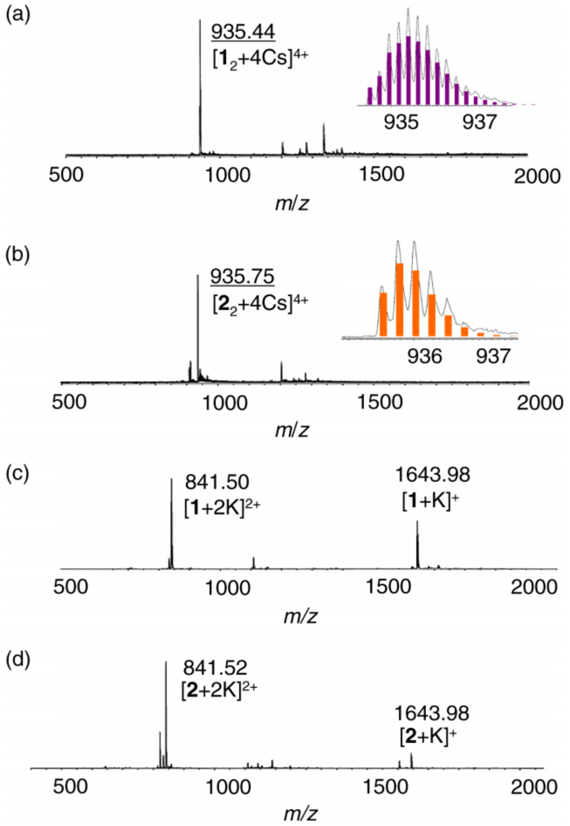

Figure 4. ESI-MS of the supramolecular form of dimetal complexes **1** and **2** in DMF. (a) **1** + 2 equiv. mol of $CsClO_4$, (b) **2** + 2 equiv. mol of $CsClO_4$, (c) **1** + 4 equiv. mol of $KClO_4$, (d) **2** + 4 equiv. mol of $KClO_4$. Calculated isotope patterns are represented by bars under a peak cluster of the parent ion.

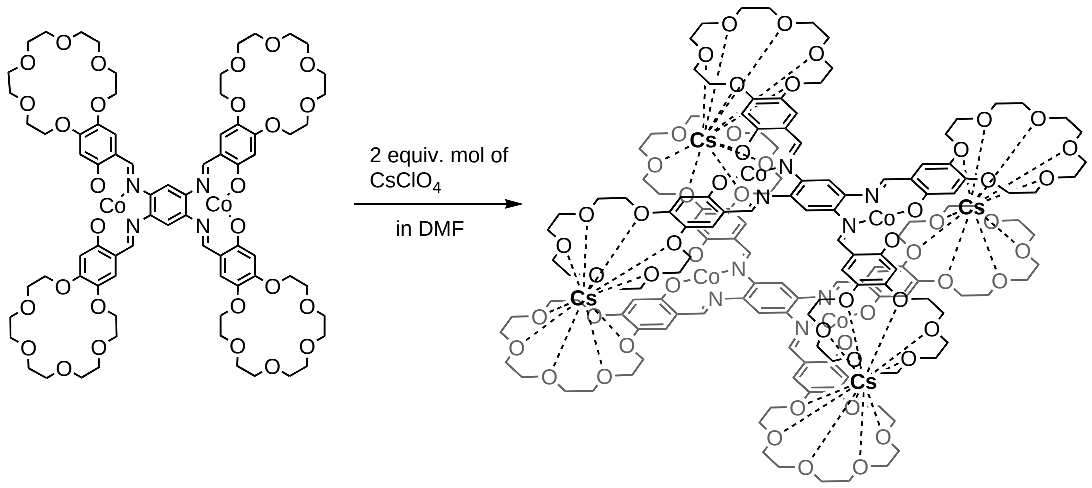

Scheme 2. Formation of face-to-face dimerised structure.

guest interaction of benzo-18-crown-6 ether with the K$^+$ ion is weak. Similar peaks at 841.52 and 1643.98 ascribed to $[\mathbf{2} + 2\mathrm{K}]^{2+}$ (M-2ClO$_4$) and $[\mathbf{2} + \mathrm{K}]^+$ (M-ClO$_4$) were observed for **2** in the presence of 4 equiv. mol of KClO$_4$ as shown in Figure 4(d). In this way, the arrangement of four benzo-18-crown-6 ether moieties in the same basic plane of the macrocycles **L1** is suitable for the face-to-face dimerised structure in **1** and **2**.

*UV–vis studies for **1** and **2***

These supramolecular assemblies of dimetal complexes (**1** and **2**) were also investigated by UV–vis spectroscopy. Both complexes showed a strong absorption around 450–550 nm ascribed to the MLCT band (*27*, *43*). These bands were changed with the addition of the Cs$^+$ ion as shown in Figure 5(a) for **1** and Figure 6(a) for **2**. The Cs$^+$ ion binding caused a hypochromic shift in the absorption band around 450–550 nm. In contrast, the UV–vis spectra of **1**

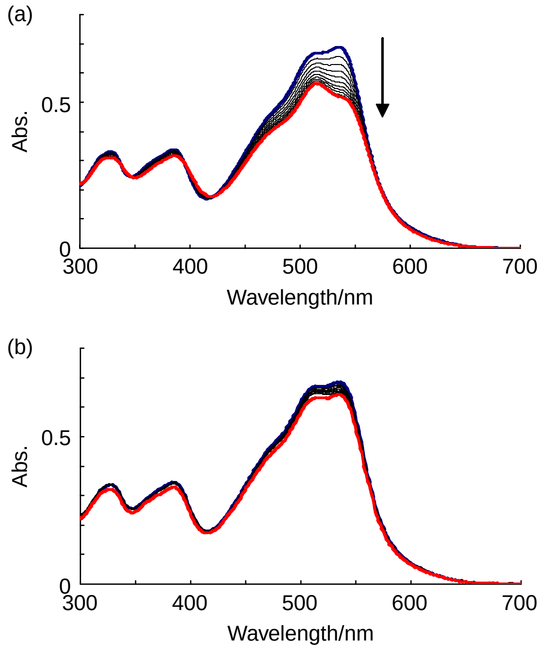

Figure 5. UV–vis absorption spectra observed during the complexation of **1** (1.0×10^{-5} M) with (a) Cs$^+$ ion (0–2 equiv. mol of CsClO$_4$) and (b) K$^+$ ion (0–4 equiv. mol of KClO$_4$) ion in DMF at 298 K.

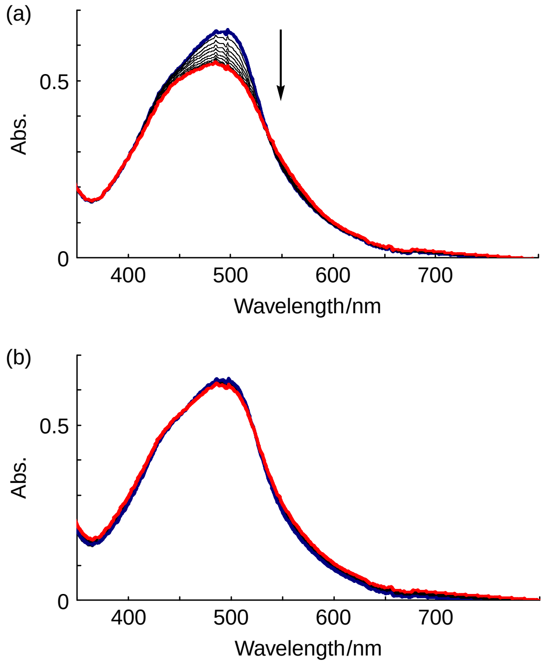

Figure 6. UV–vis absorption spectra observed during the complexation of **2** (1.0×10^{-5} M) with (a) Cs$^+$ ion (0–2 equiv. mol of CsClO$_4$) and (b) K$^+$ ion (0–4 equiv. mol of KClO$_4$) in DMF at 298 K.

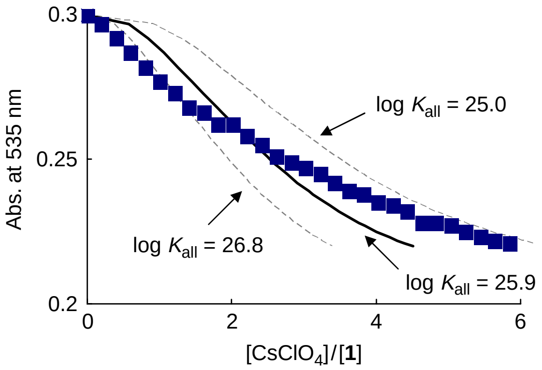

Figure 7. Absorbance changes vs. the concentration ratios of $CsClO_4$ to **1** (5.0×10^{-6} M) in DMF at 298 K: solid and dashed lines, theoretical plots; symbols, experimental data.

and **2** almost did not change with the addition of the K^+ ion as shown in Figures 5(b) and 6(b), respectively. The binding of the K^+ ion to the benzo-18-crown-6 ether moiety of **1** or **2** caused no drastic change in MLCT, whereas the binding of the Cs^+ ion significantly changed the MLCT due to the drastic structural change in the molecule. It is expected that the four-point 1:2 interaction between the Cs^+ ion and the benzo-18-crown-6 ether in the complex caused the sandwich-type structure of **1** and **2**, whereas the K^+ ion binding to the benzo-18-crown-6 ether moieties of **1** or **2** with 1:1 interaction resulted in the monomeric structure of the complex. From the UV–vis spectral change, the overall formation constant (K_{all}) of Equation (2) was determined using the reported procedure (*6*, *44*).

$$2\mathbf{1} + 4Cs^+ \rightleftharpoons (\mathbf{1})_2(Cs^+)_4 \qquad (1)$$

$$K_{all} = \frac{[(\mathbf{1})_2(Cs^+)_4]}{[\mathbf{1}]^2[Cs^+]^4} \qquad (2)$$

Theoretical plots of the absorbance changes vs. the concentration ratios of the Cs^+ ion to **1** for the various K_{all} values were constructed. The experimental points were then added to this plot, and the best fit was chosen for the K_{all} value of the assembled structure with $\log K_{all} = 25.9 \pm 0.9$ at 298 K as shown in Figure 7. In this procedure reported by Thanabal and Krishnan (*6*), the values of K can be calculated by using a variety of approximations. Therefore, the experimental plot did not exactly fit to the theoretical plot and existed in some range of the K. Thus, the overall formation constant K_{all} should be determined as some deviation using this method. Four-point sandwich structures consisting of a 2:1 host–guest interaction of the benzo-18-crown-6 ether with the Cs^+ ion afforded a significantly stable assembled structure with a high overall formation constant.

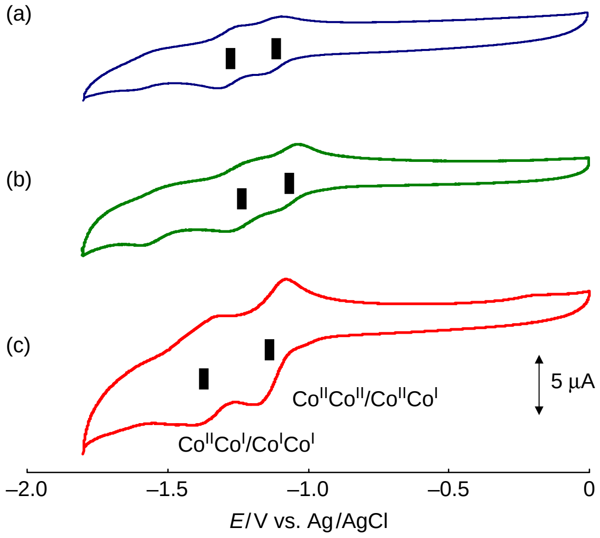

Figure 8. CVs of **2** (1.0×10^{-3} M) in DMF containing 1.0×10^{-1} M n-Bu_4NClO_4 at 298 K. (a) **2**, (b) **2** + 4 equiv. mol of $KClO_4$, (c) **2** + 2 equiv. mol of $CsClO_4$; sweep rate = 100 mV s^{-1}.

Electrochemical studies of 2

The cyclic voltammogram (CV) and differential pulse voltammogram (DPV) of the dicobalt complex **2** in *N*,*N*-dimethylformamide (DMF) at 298 K are shown in Figures 8(a) and 9(a), respectively. Two discrete redox pairs, corresponding to the $Co^{II}Co^{II}/Co^{II}Co^{I}$ and $Co^{II}Co^{I}/Co^{I}Co^{I}$ couples, were observed at -1.11 V (E_1) and -1.29 V (E_2) vs. Ag/AgCl. The two sequential reductions, E_1 and E_2, were separated by $E = E_1 - E_2 = 0.18$ V. The redox behaviour of **2** was similar to that of the dicobalt complex with the same macrocyclic ligand (two N_2O_2 cores) except for having a *t*-butyl substituent on the 3,5 position of the benzene ring in place of the benzo-18-crown-6 ether moiety (*27*). The thermodynamic significance of E can be illustrated by the comproportionation equilibrium (K_{com}) shown in Equations (3) and (4) (*27*, *45*). The K_{com} value is 1.1×10^3 at 298 K (Table 1).

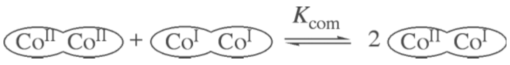

$$Co^{II}Co^{II} + Co^{I}Co^{I} \xrightleftharpoons{K_{com}} 2\,Co^{II}Co^{I} \qquad (3)$$

$$E = \frac{RT}{nF \ln K_{com}} \qquad (4)$$

We also measured the CV of **1** in DMF. Two discrete redox pairs, ascribable to the $Ni^{II}Ni^{II}/Ni^{II}Ni^{I}$ and $Ni^{II}Ni^{I}/Ni^{I}Ni^{I}$ couples, were observed around -1.29 V (E_1) and -1.61 V (E_2) vs. Ag/AgCl, respectively (data not shown). These peaks were ambiguous compared to those of **2**; therefore, we did not investigate the redox behaviour of **1** further. The CVs of the dicobalt complex **2** in the presence of guest cations, i.e. K^+ and Cs^+ ions in DMF at 298 K, are shown in Figure 8(b) and (c), respectively. The data are

Table 1. Redox potentials and K_{com} values for the dicobalt complex (**2**) in DMF.[a]

Complex	$E_{1/2}$/V vs. Ag/AgCl		K_{com}
	$\mathrm{Co^{II}Co^{II}/Co^{II}Co^{I}}$	$\mathrm{Co^{II}Co^{I}/Co^{I}Co^{I}}$	
2 ($\mathrm{Co^{II}Co^{II}}$)	− 1.11	− 1.29	1.1×10^3
2 + 4 equiv. mol of $\mathrm{KClO_4}$	− 1.06	− 1.24	1.1×10^3
2 + 2 equiv. mol of $\mathrm{CsClO_4}$	− 1.13	− 1.36	7.7×10^3

[a] Working electrode: glassy carbon, counter electrode: Pt, [complex] = 1.0×10^{-3} M, [n-$\mathrm{Bu_4NClO_4}$] = 1.0×10^{-1} M, under Ar atmosphere at 298 K. Scan rate, 100 mV/s.

summarised in Table 1. Weak peaks around − 1.6 V in Figure 8(a) and (b) are probably concerned with some oxygenated complex of **2** since CV was measured under air, the intensity of this peak became large (data not shown). In the presence of the $\mathrm{K^+}$ ion, the $\mathrm{Co^{II}Co^{II}/Co^{II}Co^{I}}$ and $\mathrm{Co^{II}Co^{I}/Co^{I}Co^{I}}$ couples were observed at − 1.06 V (E_1) and − 1.24 V (E_2) vs. Ag/AgCl, respectively, and both values were positively shifted compared to those of **2** without the guest cation due to the electron-withdrawing property of the positive $\mathrm{K^+}$ ion bound in the benzo-18-crown-6 ether moieties, although the E (= $E_1 - E_2$) and K_{com} values were the same ($E = 0.18$ V, $K_{\mathrm{com}} = 1.1 \times 10^3$ at 298 K). Thus, peripheral binding of $\mathrm{K^+}$ ions in **2** causes no drastic change in redox property probably due to keeping the monomeric structure in **2**. In contrast, the $\mathrm{Co^{II}Co^{II}/Co^{II}Co^{I}}$ and $\mathrm{Co^{II}Co^{I}/Co^{I}Co^{I}}$ couples were observed at − 1.13 V (E_1) and − 1.36 V (E_2) vs. Ag/AgCl, respectively, in the assembled structure of **2** with the $\mathrm{Cs^+}$ ion binding. The DPV clearly showed a difference between the redox behaviour of **2** in the presence of $\mathrm{K^+}$ and $\mathrm{Cs^+}$ ions. A negative shift of the second reduction peak for the face-to-

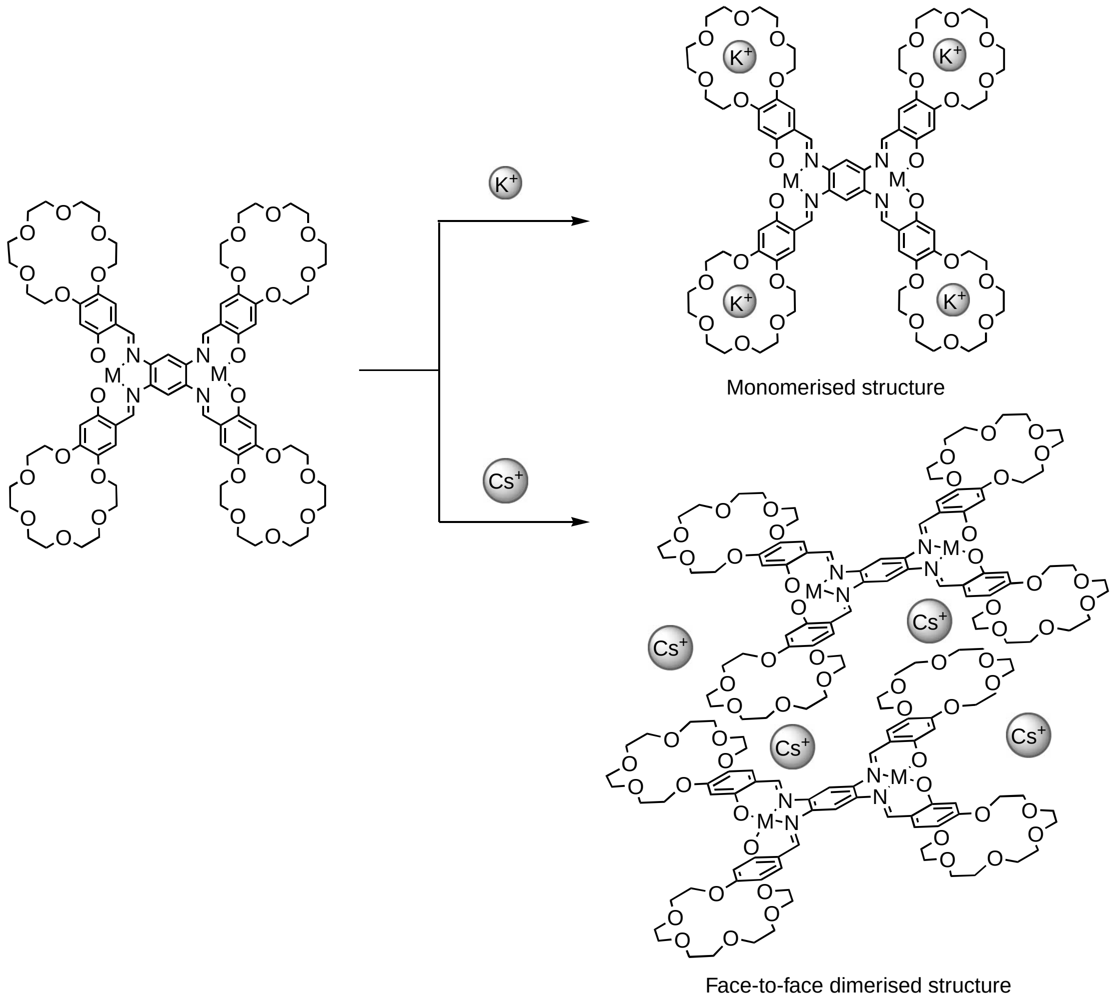

Scheme 3. Guest cation dependent host–guest complex structure.

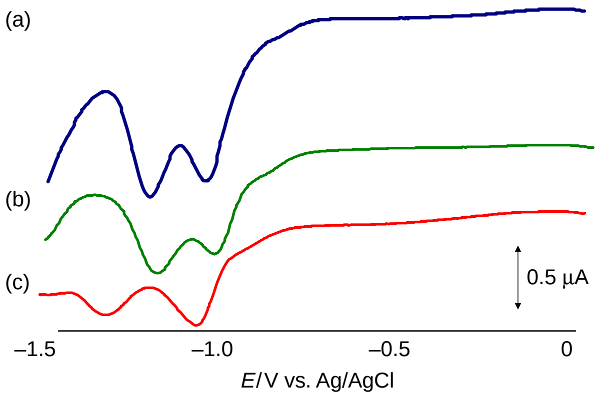

Figure 9. DPVs of **2** (1.0×10^{-3} M) in DMF containing 1.0×10^{-1} M n-Bu_4NClO_4 at 298 K. (a) **2**, (b) **2** + 4 equiv. mol of $KClO_4$, (c) **2** + 2 equiv. mol of $CsClO_4$; sweep rate = 100 mV s^{-1}.

face dimerised structure in **2** compared to those of the monomerised structure (Figure 9(a) and (b)) was observed as shown in Figure 9(c). Due to this shift, the E ($= E_1 - E_2$) and K_{com} values increased ($E = 0.23$ V, $K_{com} = 7.7 \times 10^3$ at 298 K) compared to those of **2** or **2** with the K^+ ions. The increase in K_{com} indicates a stabilisation of the mixed valence state in the assembled structure of **2** by the Cs^+ ions.

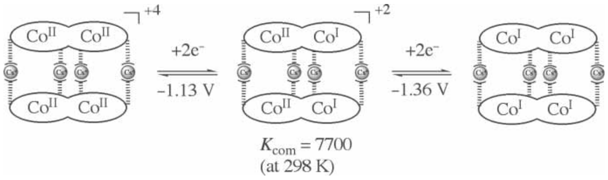

(5)

In other words, the face-to-face dimerised structure induced by the binding of the Cs^+ ions depresses the second reduction of the $Co^{II}Co^{I}$ centre. In the case of a rigid face-to-face dimerised structure, it is difficult to accommodate a large Co^{I} ion in the two N_2O_2 cores at the same time so that the second reduction shifted to the negative direction. Also, it is conceivable that the comproportionation state in **2** with the face-to-face dimerised structure may be localised in the same macrocycle unit and not located in the opposite macrocycle unit; reduction of a pair of $Co^{II}Co^{I}$ moieties should occur with no interaction. Thus, the redox wave of Figure 8(c) at -1.36 V did not split.

Concluding remarks

Supramolecular assemblies of dimetal complexes having four benzo-18-crown-6 ether moieties at the peripheral position were investigated. The dinickel and dicobalt complexes provided a unique face-to-face dimerised structure with Cs^+ ion binding as shown in Scheme 3. Multi-sandwich structures consisting of a 2:1 host–guest interaction between the benzo-18-crown-6 ether and the Cs^+ ion afforded a significantly stable assembled structure with a high overall formation constant. The results obtained here provide a new design for multi-metallic compounds that are important in many areas. We are presently exploring this molecular system in regard to various applications, such as homogeneous catalysis, magnetic materials and redox devices. These are currently in progress in our laboratory.

Experimental

All solvents and chemicals used in the syntheses were of reagent grade and were used without further purification. DMF was of spectroscopic grade (WAKO, Osaka, Japan) for the UV–vis measurements. For the electrochemical studies, DMF was stirred for 1 day in the presence of barium oxide under a nitrogen atmosphere and then distilled under reduced pressure. The distillation was performed in the absence of light, and the purified DMF was stored in a refrigerator under nitrogen in the presence of activated molecular sieves 4 Å. Tetra-n-butylammonium perchlorate (n-Bu_4NClO_4) was purchased from Nakalai Chemicals (special grade) and dried at room temperature under a vacuum before use. 4′-Hydroxy-5′-formylbenzo-18-crown-6 ether was synthesised by a reported method (*46*, *47*).

^1H, ^{13}C, 2D COSY and ROESY NMR spectra were recorded by a Bruker Avance 500 spectrometer installed at the Center of Advanced Instrumental Analysis, Kyushu University, and the chemical shifts (in parts per million) were referenced relative to the residual protic solvent peak. The UV–vis absorption spectra were measured by a Hitachi U-3300 spectrophotometer. The IR spectra were recorded by a JASCO FT-IR 460 plus KH spectrophotometer using KBr discs. The MALDI-TOF MS were obtained using a Bruker Autoflex II with dithranol as the matrix. The ESI-MS were obtained using a JEOL JMS-T100CS in DMF. The CV and DPV were obtained using a BAS CV 50 W electrochemical analyser. A three-electrode cell equipped with a 3.0 mm-diameter glassy carbon rod and 1.6 mm-diameter platinum wire as the working and counter electrodes were used, respectively. An Ag/AgCl (3.0 M NaCl) electrode served as the reference. The non-aqueous DMF solutions containing **2** (1.0×10^{-3} M) and n-Bu_4NClO_4 (1.0×10^{-1} M) were deaerated prior to each measurement, and the inside of the cell was maintained under a nitrogen atmosphere throughout each measurement. The $E_{1/2}$ value of ferrocene/ferrocenium (Fc/Fc^+) was +0.55 V vs. Ag/AgCl with this set-up.

Synthesis of dinuclear complexes

*Dinuleating ligand (**L1**)*

To a solution of 1,2,4,5-tetraaminobenzene tetrahydrochloride (90 mg, 0.32 mmol) in 5 ml of ethanol, 4′-hydroxy-5′-formylbenzo-18-crown-6 ether (670 mg, 1.88 mmol) was added under nitrogen. Five hundred microlitres of triethanolamine (3.76 mmol) were added to it and the solution was stirred for 24 h. An orange precipitate appeared by the addition of diethyl ether, which was collected by filtration, washed by dichloromethane and dried *in vacuo*. Yield: 72%. Anal. calcd for $C_{74}H_{98}N_4O_{28}$: C, 59.37; H, 6.62; N, 3.76. Found: C, 59.59; H, 6.55; N, 3.90; ^{1}H NMR (500 MHz, $CDCl_3$, 298 K): δ (ppm): 3.74–4.16 (m, 80H, crown), 6.53 (s, 4H, Ph), 6.88 (s, 4H, Ph), 7.18 (s, 2H, Ph), 8.55 (s, 4H, imine), 13.31 (s, 4H, OH); IR (KBr; ν/cm^{-1}): 1620 (C═N); MS (ESI, *m/z*): Calcd for $C_{74}H_{98}N_4NaO_{28}$: $[M + Na]^+$, 1513.6. Found: $[M + Na]^+$, 1514.2; UV–vis (in DMF): (λ_{max}/nm), 393, 421, 520_{sh}.

*Dinickel complex (**1**)*

To a solution of **L1** (51 mg, 34 mmol) in 5 ml of ethanol, $Ni(OAc)_2{\cdot}4H_2O$ (18 mg, 73 mmol) in 5 ml of ethanol was added dropwise. A dark solid immediately precipitated and the mixture was stirred at 70°C. After 3 h, the solid was collected by filtration, washed by ethanol, methanol and acetone and dried *in vacuo*. Yield: 47%. Anal. calcd for $C_{74}H_{94}N_4Ni_2O_{28}$: C, 55.38; H, 5.90; N, 3.49. Found: C, 55.13; H, 6.02; N, 3.47; ^{1}H NMR (500 MHz, DMSO-d_6, 298 K): δ (ppm): 3.54–4.05 (m, 80H, crown), 6.33 (s, 4H, Ph), 6.79 (s, 4H, Ph), 8.32 (s, 4H, imine), 8.35 (s, 2H, Ph); IR (KBr; ν/cm^{-1}): 1600 (C═N); MS (ESI, *m/z*): Calcd for $C_{74}H_{94}N_4NaNi_2O_{28}$: $[M + Na]^+$, 1625.4. Found: $[M + Na]^+$, 1626.0; UV–vis (in DMF): (λ_{max}/nm), 333, 430, 486.

*Dicobalt complex (**2**)*

All procedures were carried out using a standard Schlenk apparatus to avoid oxidation by atmospheric oxygen. To a solution of **L1** (60 mg, 40 mmol) in 5 ml of ethanol, $Co(OAc)_2{\cdot}4H_2O$ (21 mg, 86 mmol) in 5 ml of ethanol was added dropwise. A dark brown solid immediately precipitated and the mixture was stirred at 70°C. After 3 h, the solid was collected by filtration, washed by ethanol, methanol and acetone and dried *in vacuo*. Yield: 44%. Anal. calcd for $C_{74}H_{94}N_4Co_2O_{28}{\cdot}H_2O$: C, 54.75; H, 5.96; N, 3.45. Found: C, 54.74; H, 5.94; N, 3.50; IR (KBr; ν/cm^{-1}): 1590 (C═N); MS [ESI, *m/z*]: Calcd for $C_{74}H_{94}N_4O_{28}Co_2$: $[M]^+$, 1604.4. Found: $[M + H]^+$, 1605.0; UV–vis (in DMF): (λ_{max}/nm), 333, 430, 486.

Host–guest complexation behaviour

UV–vis titration

To a 1.0×10^{-5} M solution of **1** in DMF was added a stock solution of $CsClO_4$ (1.0×10^{-5} M) or $KClO_4$ (1.0×10^{-5} M) in DMF at 298 K, and the change in the UV–vis spectra of **1** was recorded at 0–2 and 0–4 equiv. mol of Cs^+ and K^+ ions, respectively (Figure 5). For the Co(II) complex **2**, the titration was carried out in a glove box to avoid air oxidation (Figure 6). For measurement of the overall formation constant (K_{all}), a 4.3×10^{-6} M solution of **1** in DMF was used at 298 K (Figure 7).

Acknowledgements

This study was partially supported by the Global COE Program 'Science for Future Molecular Systems', a Grant-in-Aid for Scientific Research on Priority Areas (452) from the Ministry of Education, Culture, Sports, Science and Technology (MEXT) of Japan and a Grant-in-Aid for Scientific Research (A) (No. 21245016) from the Japan Society for the Promotion of Science (JSPS).

References

(1) *Supramolecular Catalysis*; Piet, W.N.M., van Leeuwen, Eds.; Wiley-VCH: Weinheim, 2008.
(2) Lindoy, L.F.; Atkinson, I.M. *Self-Assembly in Supramolecular Systems*; The Royal Society of Chemistry: Cambridge, 2000.
(3) Gianneschi, N.C.; Masar, III, M.S.; Mirkin, C.A. *Acc. Chem. Res.* **2005**, *38*, 825–836.
(4) Bradshaw, J.S.; Izatt, R.M.; Bordunov, A.V.; Zhu, C.Y.; Hathaway, J.K. In *Comprehensive Supramolecular Chemistry*; Gokel, G.W., Ed.; Pergamon: Oxford, 1996; Vol. 1, pp 35–95.
(5) Gokel, G.W.; Leevy, W.M.; Weber, M.E. *Chem. Rev.* **2004**, *104*, 2723–2750.
(6) Thanabal, V.; Krishnan, V. *Inorg. Chem.* **1982**, *21*, 3606–3613.
(7) Thanabal, V.; Krishnan, V. *J. Am. Chem. Soc.* **1982**, *104*, 3643–3650.
(8) van Willigen, H.; Chandrashekar, T.K. *J. Am. Chem. Soc.* **1986**, *108*, 709–713.
(9) Sielcken, O.E.; van Tilborg, M.M.; Roks, M.F.M.; Hendriks, R.; Drenth, W.; Nolte, R.J.M. *J. Am. Chem. Soc.* **1987**, *109*, 4261–4265.
(10) Beer, P.D.; Tite, E.L.; Ibbotson, A. *J. Chem. Soc., Chem. Commun.* **1989**, 1874–1876.
(11) Sielcken, O.E.; van de Kuil, L.A.; Drenth, W.; Schoonman, J.; Nolte, R.J.M. *J. Am. Chem. Soc.* **1990**, *112*, 3086–3093.
(12) Sakata, K.; Annoura, T. *Inorg. Chim. Acta* **1990**, *176*, 123–129.
(13) Beer, P.D.; Tite, E.L.; Ibbotson, A. *J. Chem. Soc., Dalton Trans.* **1991**, 1691–1698.
(14) Van Nostrum, C.F.; Picken, S.J.; Schouten, A.-J.; Nolte, R.J.M. *J. Am. Chem. Soc.* **1995**, *117*, 9957–9965.
(15) Engelkamp, H.; Middelbeek, S.; Nolte, R.J.M. *Science* **1999**, *284*, 785–788.
(16) Engelkamp, H.; Nolte, R.J.M. *J. Porphyrins Phthalocyanines* **2000**, *4*, 454–459.
(17) Samorí, P.; Engelkamp, H.; Witte, P.de; Rowan, A.E.; Nolte, R.J.M.; Rabe, J.P. *Angew. Chem. Int. Ed.* **2001**, *40*, 2348–2350.
(18) Robertson, A.; Ikeda, M.; Takeuchi, M.; Shinkai, S. *Bull. Chem. Soc. Jpn.* **2001**, *74*, 883–888.
(19) Shinmori, H.; Yasuda, Y.; Osuka, A.; Eur *J. Org. Chem.* **2002**, 1197–1205.

(20) Liu, Y.-C.; Kuo, M.-C.; Lee, C.-W.; Liang, Y.-R.; Lee, G.-H.; Peng, S.-M.; Yeh, C.-Y. *Tetrahedron Lett.* **2008**, *49*, 7223–7226.

(21) Sandanayaka, A.S.D.; Subbaiyan, N.K.; Chitta, R.; Araki, Y.; Ito, O.; D'Souza, F. *J. Porphyrins Phthalocyanines* **2008**, *12*, 857–865.

(22) Shimakoshi, H.; Ninomiya, W.; Hisaeda, Y. *Dalton Trans.* **2001**, 1971–1974.

(23) Shimakoshi, H.; Goto, A.; Tachi, Y.; Naruta, Y.; Hisaeda, Y. *Tetrahedron Lett.* **2001**, *42*, 1949–1951.

(24) Shimakoshi, H.; Takemoto, H.; Aritome, I.; Hisaeda, Y. *Tetrahedron Lett.* **2002**, *43*, 4809–4812.

(25) Shimakoshi, H.; Kai, T.; Aritome, I.; Hisaeda, Y. *Tetrahedron Lett.* **2002**, *43*, 8261–8264.

(26) Shimakoshi, H.; Takemoto, T.; Aritome, I.; Hisaeda, Y. *Inorg. Chem.* **2005**, *44*, 9134–9136.

(27) Shimakoshi, H.; Hirose, S.; Ohba, M.; Shiga, T.; Okawa, H.; Hisaeda, Y. *Bull. Chem. Soc. Jpn.* **2005**, *78*, 1040–1046.

(28) Shimakoshi, H.; Shibata, K.; Hisaeda, Y. *Inorg. Chem.* **2009**, *48*, 1045–1052.

(29) Sessler, J.L.; Tomat, E.; Mody, T.D.; Lynch, V.M.; Veauthier, J.M.; Mirsaidov, U.; Markert, J.T. *Inorg. Chem.* **2005**, *44*, 2125–2127.

(30) Fontecha, J.B.; Goetz, S.; McKee, V. *Dalton Trans.* **2005**, 923–929.

(31) Brandt, C.D.; Kitchen, J.A.; Beckmann, U.; White, N.G.; Jameson, G.B.; Brooker, S. *Supramolecular Chem.* **2007**, *19*, 17–27.

(32) Nabeshima, T.; Akine, S. *Chem. Rec.* **2008**, *8*, 240–251.

(33) Akine, S.; Nabeshima, T. *Dalton Trans.* **2009**, 10395–10408.

(34) Nabeshima, T.; Akine, S.; Ikeda, C. *Yamamura. Chem. Lett.* **2010**, *39*, 10–16.

(35) Li, Z.; Jablonski, C. *Chem. Commun.* **1999**, 1531–1532.

(36) Ready, J.M.; Jacobsen, E.N. *Angew. Chem. Int. Ed.* **2002**, *41*, 1374–1377.

(37) Haak, R.M.; Belmonte, M.M.; Escudero-Adán, E.C.; Benet-Buchholz, J.; Kleij, A.W. *Dalton Trans.* **2010**, *39*, 593–602.

(38) Okawa, H.; Furutachi, H.; Fenton, D.E. *Coord. Chem. Rev.* **1998**, *174*, 51–75.

(39) Hui, J.K.-H.; Yu, Zhen; MacLachlan, M.J. *Angew. Chem. Int. Ed.* **2007**, *46*, 7980–7983.

(40) Frischmann, P.D.; MacLachlan, M.J. *Chem. Commun.* **2007**, 4480–4482.

(41) Chen, L.; Wang, L.; Gao, X.; Nagase, S.; Honsho, Y.; Saeki, A.; Seki, S.; Jiang, D. *Chem. Commun.* **2009**, 3119–3121.

(42) Akine, S.; Utsuno, F.; Nabeshima, T. *Chem. Commun.* **2010**, *46*, 1029–1301.

(43) Merrell, P.H.; Abrams, M. *Inorg. Chim. Acta.* **1979**, *32*, 93–98.

(44) Chernyad'ev, A. Yu; Logacheva, N.M.; Tsivadze, A.Y. *Russ. J. Inorg. Chem.* **2006**, *51*, 720–723.

(45) Gagné, R.R.; Spiro, C.L.; Smith, T.J.; Hamann, C.A.; Thies, W.R.; Shiemke, A.K. *J. Am. Chem. Soc.* **1981**, *103*, 4073–4081.

(46) Wada, F.; Arata, R.; Goto, T.; Kikukawa, K.; Matsuda, T. *Bull. Chem. Soc. Jpn.* **1980**, *53*, 2061–2063.

(47) Can, S.; Bekâroglu, Ö. *J. Chem. Soc. Dalton Trans.* **1988**, 2831–2835.